Evidences of Sub-Optimal Photogrammetric Modelling In RPAS-based Aerial Surveys

Pascal Sirguey, Julien Boeuf, Ryan Cambridge and Steven Mills
University of Otago
Dunedin, New Zealand
pascal.sirguey@otago.ac.nz

Keywords: photogrammetry, RPAS, self-calibration, digital elevation model, accuracy

Introduction

Remotely Piloted Aircraft Systems (RPAS) are revolutionizing aerial mapping and find many successful applications in surveying and environmental monitoring. These new platforms, often associated with consumer-grade digital cameras, enable the collection of overlapping imagery at a relatively low financial and logistical cost. Digital technology associated with progress in computer vision (Hartley and Zisserman 2003) and the increasing affordability of computing power have simplified and democratised the once complex photogrammetric process (Calomina and Molina 2014). The plethora of platforms available and photogrammetric software priced for all budgets promise any users to ability to produce dense point clouds and generate ortho-photos with resolution and accuracies once achievable by specialized surveyors only.

Ultimately, the accuracy of positioning points in 3D with photogrammetry boils down to reprojecting into 3D space the rays of light of which each image pixel is a record. This requires modelling the trajectory of the light ray outside and inside the camera using exterior and interior orientation parameters (E/IOPs), respectively (Mickail et al. 2001). Despite the apparent simplicity of capturing and processing aerial imagery into dense 3D models with the expectation of centimetre accuracy, the photogrammetric process still relies on highly technical steps making the determination of the required IOPs and EOPs not as trivial as it seems.

Traditional photogrammetry has long relied on specialised, purposely-built, metric cameras whose IOPs are calibrated separately, leaving only the EOPs of each image to be determined by the bundle block adjustment (BBA). Alternatively, recent applications of photogrammetry with consumer grade cameras by non-expert users often relies on a self-calibration approach whereby IOPs and EOPs are solved concurrently as part of the same BBA (Rosnell and Honkavaara 2012). However, this process often ignores that the photogrammetric network of images captured in RPAS operations rarely has the geometric strength to allow the self-calibration approach to find the optimal solution to the global problem (Brown 1989). This is a pre-requisite for the robustness of the photogrammetric model, its relative insensitivity to the network of ground control points (GCPs), allowing fieldwork to be reduced, and an accuracy extending at relatively great distance from GCPs. The risk of a sub-optimal adjustment, whereby a local optimum of the IOPs and EOPs is found but the correlations between them not fully and unambiguously resolved make errors in the modelling of the IOPs propagate in the EOPs.

Un-modelled camera distortions thus translate into large scale distortions of the output terrain that can severely compromise or restrict its validity.

This study explores how RPAS-based survey can yield sub-optimal solutions to the photogrammetric problem by processing the same dataset with different photogrammetry software and under various scenarios of ground control network. Beyond the mere residuals associated with GCPs and check points (CPs), this study examines and reports on the variability associated with the IOPs and EOPs under each scenario to characterise better the strengths and limitations of RPAS-based surveys.

Data and Methods

Imagery

We conducted a case study over farmland on Okia Flat (Otago Peninsula, New Zealand) using a Trimble UX5 fixed-wing RPAS. The area to be covered was approximately 280 ha with elevation differences ranging from near sea level to 15m above. The terrain undulates to a significant degree, consistent with former sand dunes. Three flights of 40 minutes at an altitude of 400ft agl were required to cover the area although data from a single flight only (ca. 1.6 km^2) were considered in this study to reduce the computing time. The UX5 embarks a Sony Alpha NEX-5R 16.6MP mirror-less SLR camera equipped with a Voigtländer 15mm f/4.5 lens whose focus ring is fastened at infinity and resolving 3.6cm at 400ft. Photos were captured with 80% forward and sideward overlap resulting in 1374 images.

Ground Control Points

Signalled GCPs were made of 60x60cm floor mats painted with a contrasted photogrammetric pattern. 44 GCPs were evenly distributed in the area and surveyed with GNSS RTK yielding centimetre errors on the fixed solution. 25 of them were visible in the single flight considered here. 11 natural features (NF) were also surveyed to be used as additional CPs.

Photogrammetric Software

The photogrammetric processing was completed using two leading software packages, namely Trimble Business Centre v3.4 (TBC) and Pix4DmapperPro v2.1. As the standard package to process UX5 data, TBC inherits the triangulation engine of Inpho UASMaster customized for the UX5 hardware. It offers limited or no adjustment options and always enforces self-calibration from a set of initial IOPs determined by the manufacturer. Alternatively, Pix4D allows greater customization of the adjustment with selective weighting of the parameters (i.e., GCPs accuracy vs. initial EOPs), as well as the option to disable the self-calibration. For processing in Pix4D, initial IOPs were set to match those used in TBC. Initial EOPs, including location (GPS C/A code) and attitude angles were obtained from the flight log.

Triangulation Scenarios and Performance Metrics

In order to characterize the robustness of the BBA solution, eight scenarios involving a varying number and placement of GCPs were tested (Fig. 1). The fully controlled scenario

1 was assumed to be the closest from reality and used as a reference against which departure in IOPs and EOPs were compared.

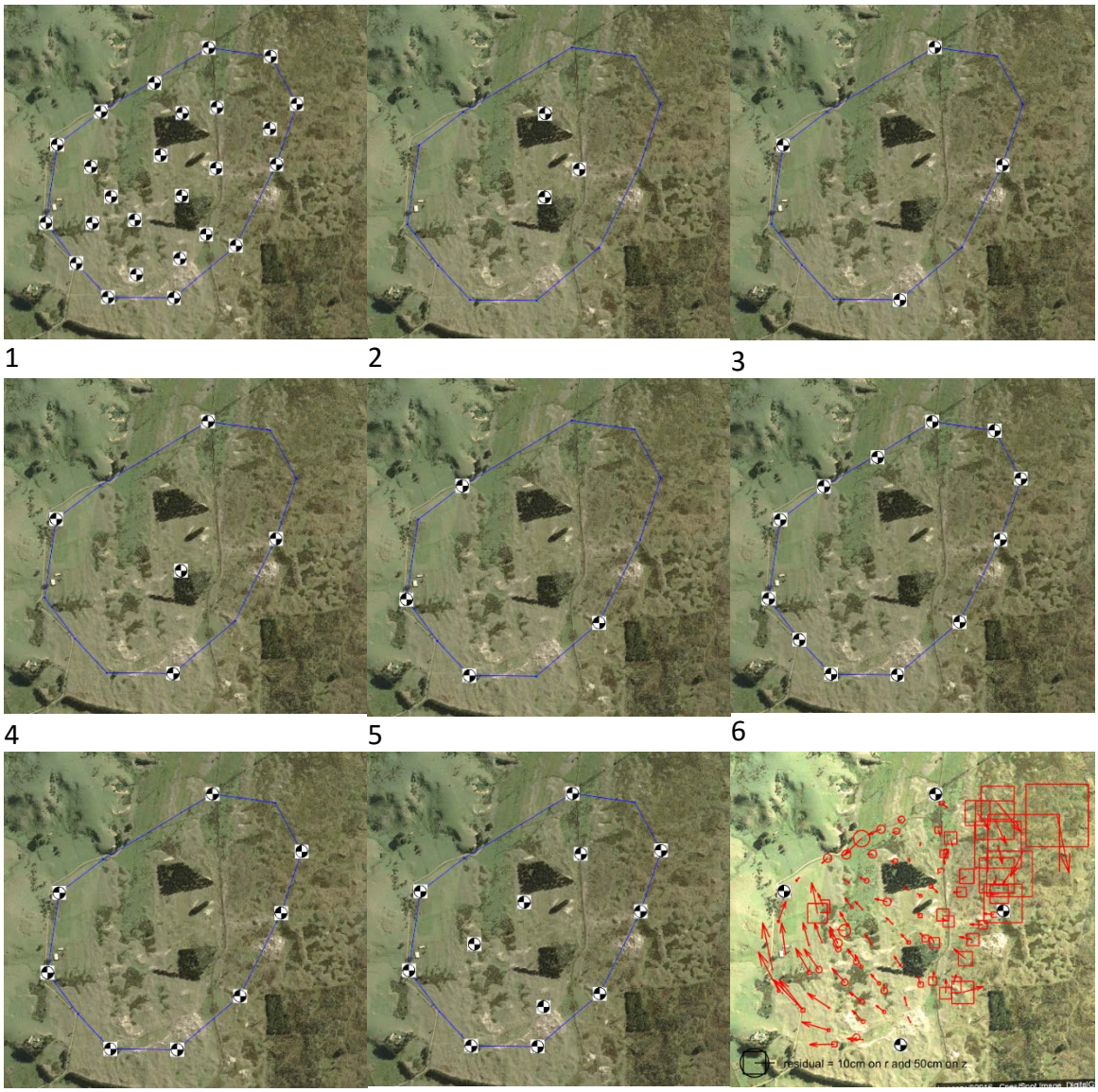

Figure 1. The various scenarios of ground control. Note the scenario (1) with all 25 signalled points as GCPs providing the reference case against which other scenarios are tested. The lower right image illustrates the result of the residual associated with the set of CPs (scenario 3, Pix4D).

In order to visualise better the possible patterns of distortion between scenarios and support stronger statistics, a set of 54 synthetic check points (SCPs) was determined by resecting 3D coordinates from the reference scenario 1 (see Fig. 1).

Scenarios were compared by computing the RMS residuals in XYZ directions for each set of points. The mean and standard deviation associated with the set of IOPs determined by each software across scenarios were compared to assess intra- and extra- software consistency. Finally, EOPs between the reference scenario of each software and selected

scenarios associated with identical software were compared to characterise the robustness and consistency of the solutions.

Table 1. Residuals for each scenarios and each type of points. All values are in mm.

	Scenario	n GCP	GCP as control (n)			CP (25 - n)			NF (n = 11)			SCP (n = 54)		
			X	Y	Z	X	Y	Z	X	Y	Z	X	Y	Z
TBC	1	25	8	6	1				58	28	24			
	2	3	6	10	0	294	270	255	227	290	350	207	184	142
	3	4	3	7	1	86	105	98	138	252	140	66	61	70
	4	5	3	8	1	76	101	50	145	179	81	45	53	27
	5	4	5	8	1	323	171	315	165	341	701	281	171	217
	6	12	11	7	1	37	23	16	69	32	29	13	9	10
	7	8	12	9	1	44	39	18	64	58	29	20	19	10
	8	12	9	7	1	47	40	21	62	57	29	18	15	9
Pix4D	1	25	22	18	41				45	40	246			
	2	3	9	12	0	89	66	1357	111	79	1375	56	46	921
	3	4	8	8	6	59	83	459	45	91	497	42	56	282
	4	5	12	10	6	57	75	482	45	91	528	33	45	286
	5	4	9	11	2	92	88	1303	121	114	1488	70	69	931
	6	12	25	17	22	24	33	240	49	37	336	11	11	177
	7	8	23	18	17	23	37	702	41	45	813	10	14	659
	8	12	24	18	22	24	37	228	42	42	372	8	11	127

Results and Discussion

Overall Assessment

Table 1 shows the overall performance associated with each scenario and software. TBC yields smaller residuals on GCPs. Results on the sets of independent points exhibit a consistent result whereby Pix4D achieved consistently better planimetric accuracy, while TBC outperforms Pix4D on height. Strong departures with poorly constrained scenarios 2, 3, and 5 show that both software fail to find optimal solutions. Figure 2 further shows that such departure is correlated to the distance from the nearest control point with significantly greater divergence outside the convex polygon formed by GCPs. This dependence to distance to GCPs show that the terrain model quickly becomes unreliable outside the support of GCPs. The sub-optimality of the solution is confirmed by observations of systematic patterns in the norm and direction of residuals from the set of SCPs (Fig. 1).

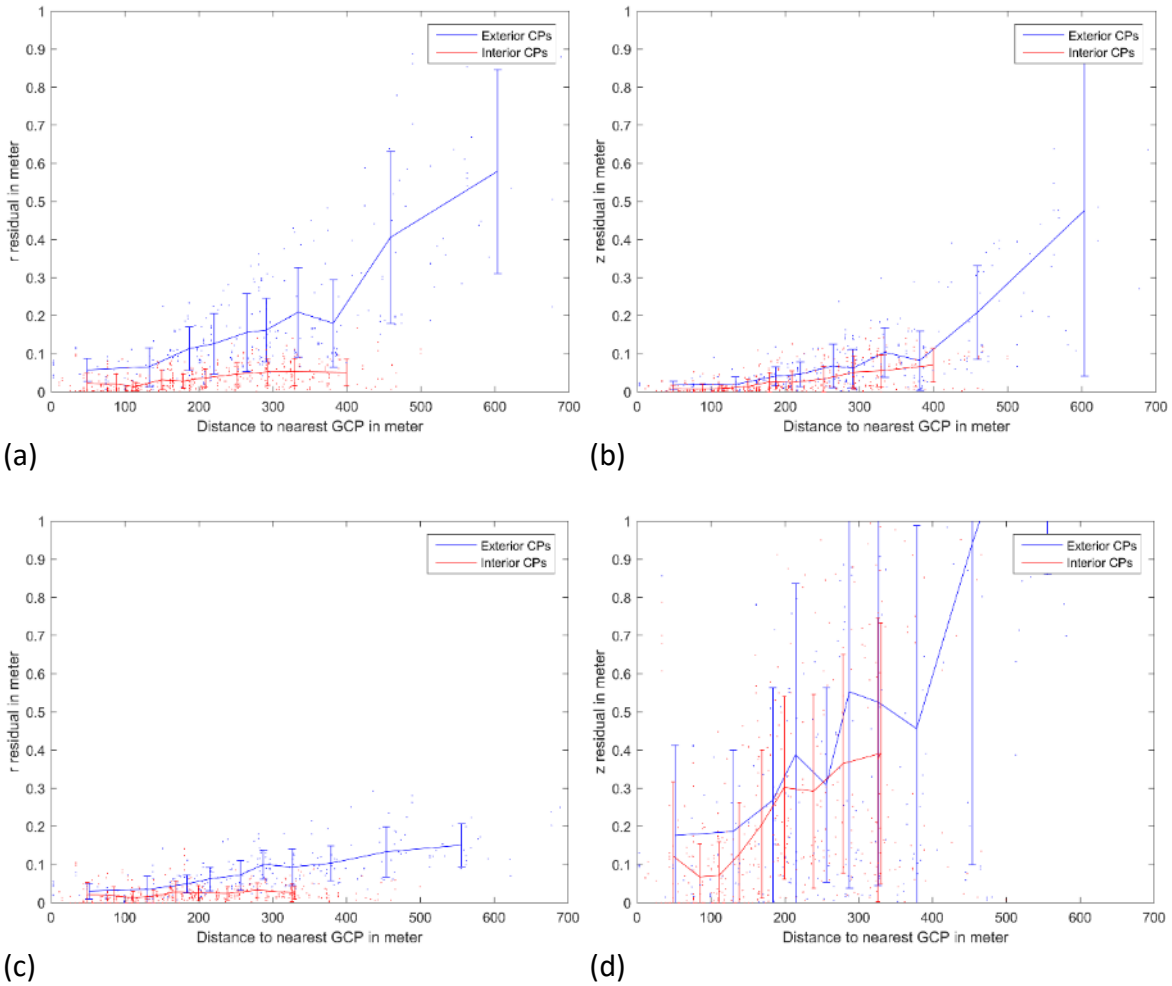

Figure 2. Magnitude of the planimetric (left) and elevation (right) residual as a function of distance to the nearest GCP for TBC (top) and Pix4D (bottom).

IOPs

Table 2 and Figure 3 demonstrates that both software determine very stable IOPs, regardless of the scenario. This suggests a relatively high weighting of the initial IOPs in the BBA possibly compounded with a weak photogrammetric network preventing each software to refine IOPs. The slightly longer focal length (~1‰) determined by Pix4D is compensated by a higher flying height due to the direct correlation between both parameters. Lens distortion parameters determined by both software appeared to be very similar.

Table 2. Internal Orientation Parameters.

	Pix4D		TBC	
	Mean	STDev	Mean	STDev
PPA X (mm)	8.583E-03	2.53E-04	8.738E-03	1.67E-03
PPA Y (mm)	-1.574E-02	3.61E-04	-1.393E-02	1.62E-03
Focale length (mm)	15.464	2.26E-03	15.454	2.44E-03
K1 (m^{-2})	-1.981E-04	1.35E-06	-1.985E-04	8.46E-07
K2 (m^{-4})	6.440E-07	5.83E-09	6.477E-07	6.12E-09

K3 (m^{-6})	-7.725E-10	2.10E-11	-7.612E-10	2.38E-11
T1 (m^{-1})	-3.913E-05	5.09E-07	-3.748E-05	3.58E-07
T2 (m^{-1})	8.701E-05	5.55E-08	8.735E-05	1.34E-07

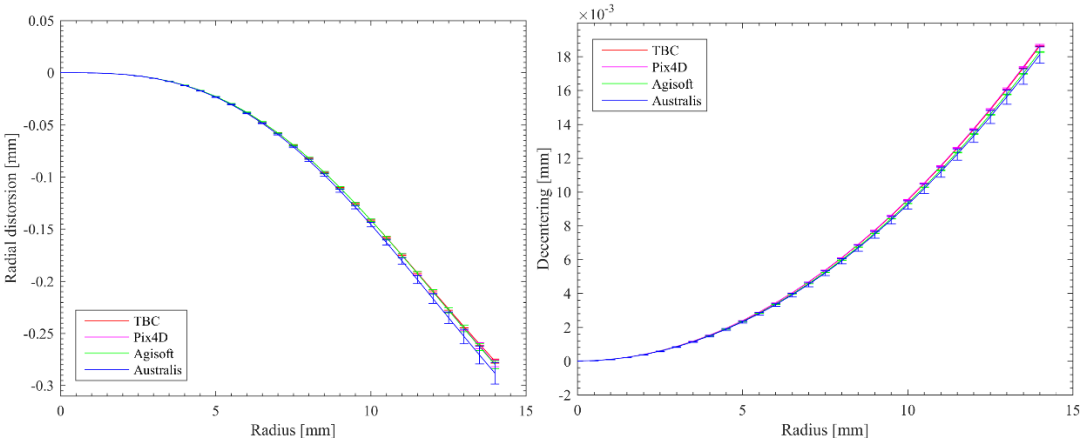

Figure 3. Mean radial (left) and decentering (right) distortion curves associated with all scenarios for each software. The error bar depicts the variance associated with the modelled distortion.

EOPs

Figure 4 (a) show that inside the convex polygon supported by the GCPs, TBC and Pix4D determine planimetric coordinates of optical centres consistent within ~20cm. EOPs then diverge quickly outside the support of GCPs with discrepancies exhibiting a period matching the flight strips. Pix4D models the camera ~10cm higher than TBC in consistence with its longer modelled focal length. Figure 4 (b) and Figure 5 shows that departures between each software worsens significantly in less controlled scenario 5. Both cases exhibit a marked, yet repeatable, altitudinal drift between solutions outside the support from GCPs. Figure 4 (b and c) illustrates how much EOPs can vary with the same software under different scenarios. This confirms the strong sensitivity to the control network and the failure of one and probably both software to find the optimal solution to the global problem.

Conclusion

This study provides evidence of the potential failure by two leading software solutions to determine optimal parameters of a photogrammetric model captured by a RPAS system. Despite the similar and repetitive estimations IOPs, both software diverge significantly in their estimation of EOPs under the same control scenarios, possibly due to contrasting optimisation techniques in the BBA. This yields systematic and spatially structured distortion patterns in the terrain model that may make the assessment of residuals from limited control/check network misleading about the true accuracy of the output model. Our results also confirm that solution of the photogrammetric problem becomes highly sensitive to the control network, with distance to the nearest GCP and whether being inside or outside the support of the control network governing the accuracy.

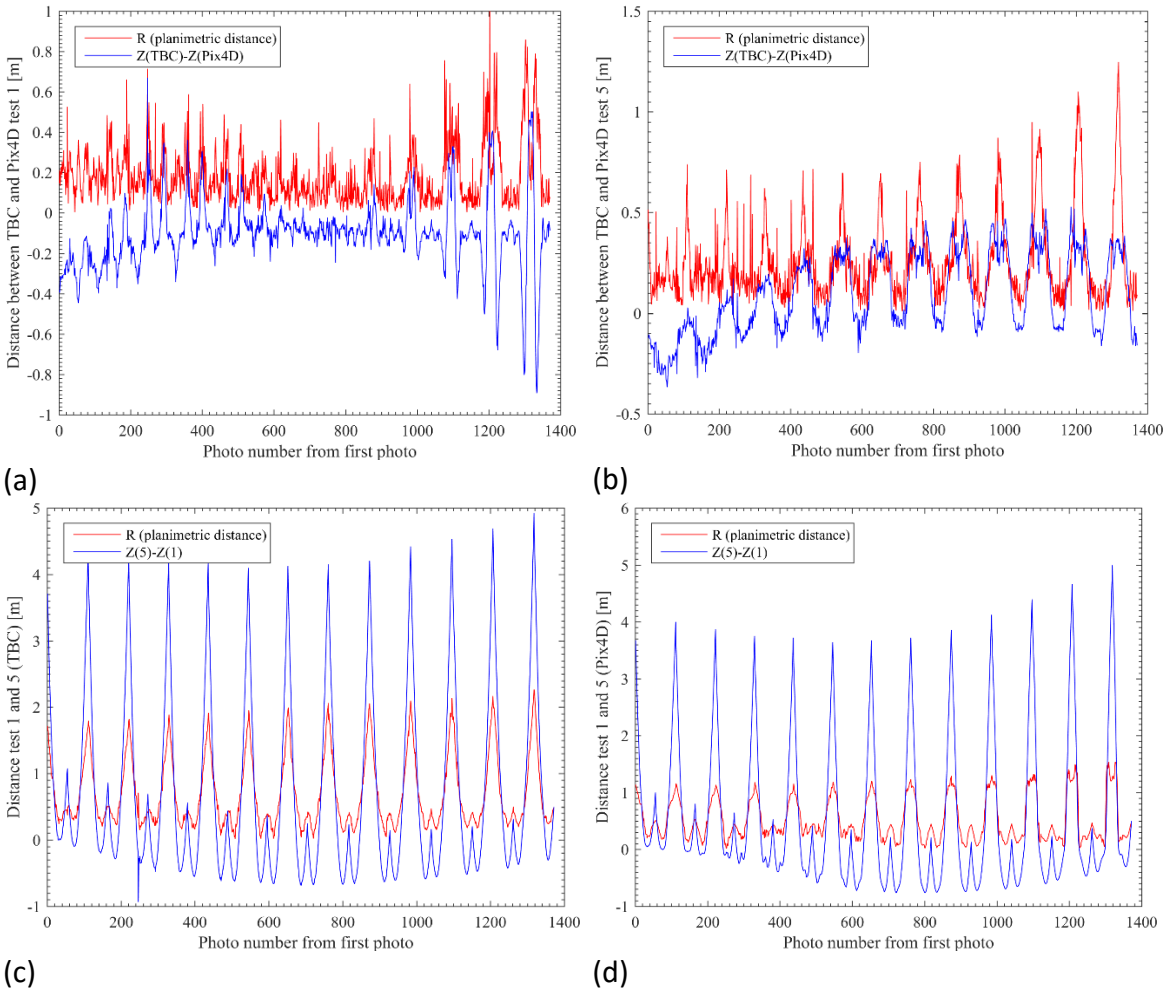

Figure 4. Planimetric and altitudinal separation between EOPs from TBC and Pix4D for the scenarios 1 (a) and 5 (b). Planimetric and altitudinal separation between EOPs for scenarios 1 and 5 for TBC (c) and Pix4D (d).

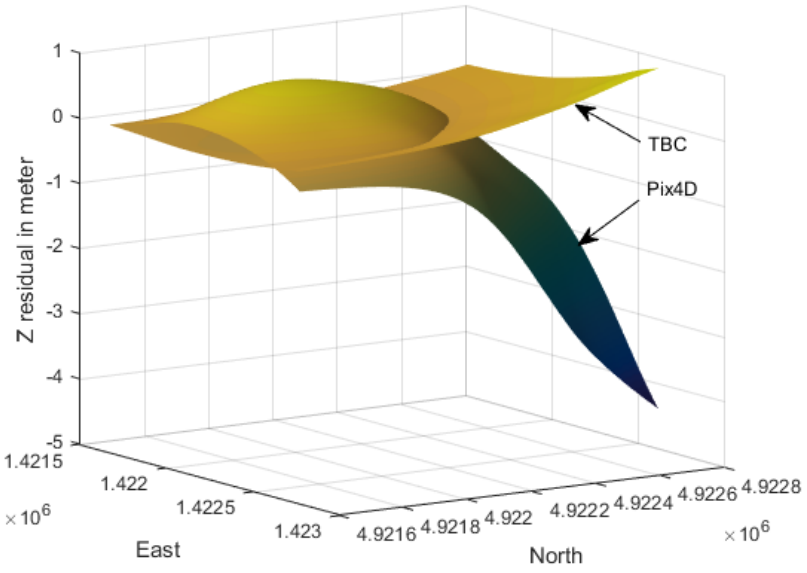

Figure 5. Comparison of the trend of residuals between TBC and Pix4D in the scenario 5.

Acknowledgments

The authors thank Jason Clearwater for authorizing access to his farm. Ryan Cambridge was supported by a summer bursary grant from LINZ. Julien Boeuf was supported by a travel grant from the Région Rhône-Alpes, France.

References

Brown D. (1989). A strategy for multi-camera on-the-job self-calibration, *Schriftenreihe 14, Institut für photogrammetrie der Universitðt Stuttgart,* 302, 9-21.

Colomina I. and Molina P. (2014). Unmanned aerial systems for photogrammetry and remote sensing: A review, *ISPRS Journal of Photogrammetry and Remote Sensing,* 92(0), 79-97.

Hartley R. and Zisserman A. (2003). *Multiple View Geometry in Computer Vision*, Cambridge University Press, Cambridge.

Mikhail E. M., Bethel J. S. and McGlone J. C. (2001). *Introduction to Modern Photogrammetry*, John Wiley & Sons, New York.

Rosnell T. and Honkavaara E. (2012). Point cloud generation from aerial image data acquired by a quadrocopter type micro unmanned aerial vehicle and a digital still camera, *Sensors,* 12(1), 453-480.